Curvature Instability in a Chiral Amphiphile Self-Assembly

Lior Ziserman,[1] Amram Mor,[1] Daniel Harries,[2,*] and Dganit Danino[1,3,†]

[1]Department of Biotechnology and Food Engineering, Technion-Israel Institute of Technology, Haifa 32000, Israel
[2]Institute of Chemistry and The Fritz Haber Research Center, The Hebrew University, Jerusalem 91904, Israel
[3]The Russell Berrie Nanotechnology Institute, Technion-Israel Institute of Technology, Haifa 32000, Israel

(Received 28 December 2010; published 9 June 2011)

We present the first experimental evidence for the morphological transition from twisted to helical ribbons in amphiphile aggregates. This transition, from structures possessing negative Gaussian curvature to helically curved structures, is shown to be directly linked to ribbon width. Time-resolved cryotransmission electron microscopy images of a peptidomimetic amphiphile further capture the dynamic transformation between the two geometries along a single ribbon unit. Quantitative analysis indicates that both ribbon width and pitch grow with ribbon maturation, maintaining a constant ratio.

DOI: 10.1103/PhysRevLett.106.238105 PACS numbers: 87.14.ef, 64.75.Yz, 87.15.bk

From toxic amyloid fibrils linked to neurodegenerative diseases [1] to DNA that encodes the information of life, chirality is inherent to all basic biomacromolecules: nucleic acids, proteins, polysaccharides, and phospholipids [2,3]. The self-assembly of chiral molecules is evident in a variety of forms, including the organization of cellulose fibers in plant cell walls [4], as well as multicomponent lipid mixtures that form filaments, helical ribbons, and tubes in nucleating bile and gallstones [5–7]. Similar structures have been gaining interest for technological applications, such as the application of nanotubes as drug delivery and slow-release nanometric containers [8] or as templates for production of conductive metal nanowires [9]. Thus, understanding the elements and forces that lead to specific forms of chiral self-assembly is key to controlling selective direct assembly.

Chiral amphiphiles form a particularly interesting class of molecules, because they are able to self-assemble into a variety of structures with a wide range of dimensionalities, ranging from 0D spherical micelles through 1D cylindrical micelles to extended 2D sheets. Clearly, these different structures also possess distinct material properties, such as elasticity. Furthermore, under different solution conditions, the very same molecules may organize into a range of chiral aggregates, such as ribbons and nanotubes (Fig. 1). Here we show that this unique property opens the possibility to follow changes in structure and material properties of chiral self-assembly, by using the temporal evolution of amphiphile assembly.

Ribbons are among the most common and important structures of assembled chiral amphiphilic molecules. Two distinct classes of structures are twisted ribbons with negative Gaussian curvature, and helical (spiral) ribbons with cylindrical bending characterized by zero Gaussian curvature and significant mean curvature (Fig. 1) [10]. What drives the formation of twisted versus helical assemblies is a delicate interplay between different elastic forces and chirality. It has been shown that if bending deformations are allowed (low mean bending modulus), spiral ribbons will dominate, whereas if Gaussian curvature and extensions within a ribbon are allowed (i.e., low saddle-splay modulus or low enough edge energy), twisted structure will be preferred. Selinger and co-workers [11] were the first to suggest theoretically a possible transformation between twisted and helical ribbons. Using Monte Carlo simulations, they showed that aggregate curvature may change smoothly from Gaussian to cylindrical as a function of elastic moduli [11,12]. Ghafouri and Bruinsma proposed that *there is* in fact a sharp transition point between twisted and spiral ribbons that depends on ribbon width [13]. Specifically, ribbon widening lowers the relative edge energy cost per unit length but substantially increases the energetic cost of twist due to an increase in the stretching energy required for deformation.

This balance of forces was predicted to lead to a nonmonotonic change in ribbon energy as a function of ribbon

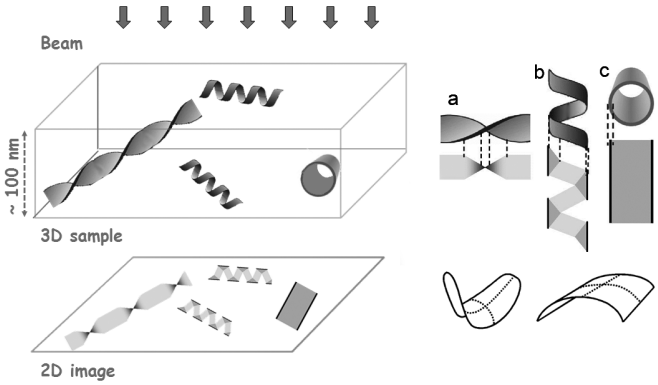

FIG. 1. Schematic of a typical cryo-TEM specimen and the corresponding image. Specimen thickness ranges between 80 and 150 nm. The right panel displays twisted ribbons (a), helical ribbons (b), and nanotubes (c), together with their appearance in the projected images, and the corresponding Gaussian (left) and bending (right) curvatures.

width, showing a minimum at an intermediate width followed by energy barrier and finally decay as the ribbon further widens. Moreover, depending on the so-called Föppl–von Kármán number (a dimensionless ratio of the stretching energy per unit area of ribbon over the characteristic lateral bending energy per unit area), the ribbon morphology corresponds to twisted ribbons when stretching energy is low and to spiral ribbons at large ribbon width where stretching energy is much higher than bending [13]. A critical value of this parameter separates regimes where twisted versus helical ribbons are stable.

Despite these theoretical predictions, and the variety of self-assembling and other materials that have been shown to reside in twisted or helical structures, so far there has not been any experimental proof relating the morphology of the ribbons to their width. In this Letter, we provide the first direct evidence in an amino-acid-based amphiphilic system that twisted ribbons are precursors of cylindrical (helical) ribbons. Moreover, by cryogenic-transmission electron microscopy (cryo-TEM; see Fig. 1) we explicitly capture the dynamic transition between the two ribbon morphologies, twisted and helical, along *a single ribbon* and quantitatively link the curvature and shape transformation with ribbon width. This has allowed us to isolate the ribbon width as the relevant physical parameter that determines the preferred shape.

Our system is composed of a dilute aqueous solution of a short lipo-amino acid, *N*-lauryl-lysyl-aminolauryl-lysine-amide, referred to as C_{12}-β_{12} [Fig. 2(a)]. This compound

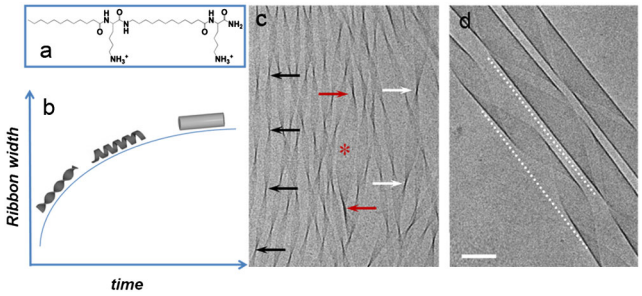

FIG. 2 (color online). Temporal and structural evolution of C_{12}-β_{12} assembly. (a) Molecular structure of C_{12}-β_{12}. (b) Qualitative description of the time-dependent evolution of structures (width and morphology): Twisted ribbons populate the solution after overnight incubation as shown in (c), helical ribbons form following aging for 4 weeks as shown in (d), and nanotubes form after $\approx$ 4 months (not shown). The black arrows in (c) follow the nodes of constant pitch along one narrow twisted ribbon, while the white arrows mark the larger pitch of another, wider ribbon of the same geometry. The red asterisk and arrows mark one helical ribbon existing in the field of twisted ribbons. The dashed lines in (d) are located left and below 2 neighboring helical ribbon captured at different stages of their development towards closed nanotubes. Each line follows 2 pitch lengths (complete turns). Note that the two molecular complexes have different diameter as well as different pitch. Bar = 100 nm.

belongs to a synthetic library of pseudopeptides termed oligo-acyl-lysyl, designed to mimic the structure and function of host defense peptides [14]. Their general sequence comprises tandem repeats of hydrophobic and hydrophilic motifs, specifically, lauryl and lysyl residues, linked by amide bonds. As shown in Fig. 2(a), C_{12}-β_{12} is made of two such repeats. This molecule may also be regarded as a special form of a head-to-tail Gemini amphiphile [15,16], where one hydrophobic moiety acts as an amphiphilic tail, while the other is a spacer.

Indeed, beside its antimicrobial effects, [17,18], we find that C_{12}-β_{12} in solution undergoes a slow aggregation process, starting with the creation of nanofibers, which transform into twisted ribbons, then gradually into helical ribbons, and eventually into closed nanotubes of 70–120 nm in diameter and several microns in length. This process is driven by the tendency to lower the energy associated with ribbon edges. The assembly process and the molecular model are presented in detail elsewhere [19].

Here, we focus on the ribbon morphology and on the unique ability of C_{12}-β_{12} assemblies to slowly transform from twisted [Fig. 2(c)] to helically coiled structures [Fig. 2(d)] as the ribbons expand in width. Quantitative analysis of ribbon population was performed by measuring the pitch length (p) and ribbon width (w) for 917 identified segments of one pitch length, belonging to 382 twisted and helical ribbons, at various time points along their maturation path (aging time ranged from 30 min to 4 weeks). For this analysis, all possible pitch and width values of the ribbons in the field of view were measured.

Clearly, the amphiphilic system reaches full equilibrium only at long times of several months. Over this time span, the ribbons widen and eventually close to tubes. In contrast, the dynamics of aggregate remodeling and bending are much faster, resulting in a significant separation in widening versus deformation relaxation time scales. This allows us to assume that, at any given time during the aggregation process, the aggregate structure represents an intermediate that is at local equilibrium with respect to the faster elastic degrees of freedom, while it is overall metastable with respect to ribbon width since it slowly continues to grow. Therefore, we suggest that ribbons seen in cryo-TEM images have elastically deformed to acquire the minimum energy for their given width at the time of capture.

This assumption allows us to determine the correlation of width and morphology, as shown in Fig. 2. At early times, thin twisted ribbons of a few nanometers ($w < 10$ nm) in width exist almost exclusively. As time progresses, the ribbons become wider, and for the majority of structures ($> 92\%$ of measurements, grouped as class I in Fig. 3) we find that twisted ribbons with saddlelike curvature (blue symbols) that dominate at early times evolve into helical ribbons (red symbols) at long incubation time. The transition in curvature occurs at a

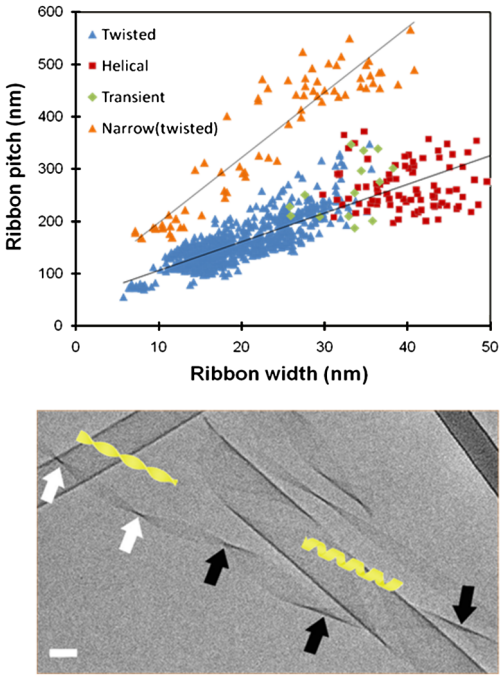

FIG. 3 (color online). Morphology transition in C_{12}-β_{12} solutions. Upper panel: Statistical analysis of the variations of ribbon pitch with ribbon width. Note that p varies linearly with w for the two classes. The majority of structures ($> 92\%$) are grouped in class I; these create narrow twisted ribbons at early time points, which transition into helices as ribbons get wider (w transition $= 30 \pm 4$ nm) with aging. Class II structures are characterized by a longer pitch (smaller w/p); these assemblies remain twisted over the entire study period. Lower panel: Cryo-TEM image showing a ribbon that becomes wider along its length, concurrently transitioning from twisted (white arrows) to helical (black arrows). Bar = 25 nm.

well-defined width of $w = 30 \pm 4$ nm, and, for all larger widths in class I, the preferred curvature remains cylindrical. Thus, beyond the transition point, the wider the ribbon, the lower the free energy, thereby making the process of ''nucleating'' ribbons into tubes more likely.

Strikingly, in a number of structures we captured the dynamic transition between twisted and helical curvatures (green symbols) along a single ribbon. One clear example is presented in Fig. 3 (lower panel); highlighted with arrows is a nonuniform ribbon that gradually expands in width along its length, displaying saddlelike curvature (barber-pole structure) at the thin width region and helical at the thick.

Evidently, as shown in Fig. 3, not only the ribbon width increases but also the pitch. Moreover, irrespective of ribbon curvature and structure, ribbon width w seems to vary almost linearly with its pitch p.

Therefore, it seems that an additional parameter, the ratio of width to pitch (w/p), plays a significant role in the transition. Interestingly, this ratio could be expected to signify relative bend versus twist (or stretching) energies; for example, large width combined with large pitch would signify large bending resulting from prohibitively large twist energies. Therefore, this ratio may be a useful parameter that reflects the elastic material properties (somewhat analogous to the Föppl–von Kármán parameter). Specifically, changes in w/p may indicate different molecular packing or different aggregate arrangements. Furthermore, different w/p ratios may correlate with different transition points between twisted and helical forms.

Two very different contributions lead to the scatter of points seen in Fig. 3. One is an inevitable experimental error associated with the fact that in the cryo-TEM images we measure the 2D projections of the structures occupying the volume (for specimen details, see Fig. 1). The second, and perhaps more meaningful contribution, results from true inherent fluctuations of the assembly that lead to a spread in the pitch length. In fact, for 1D systems that show growth primarily in one direction (such as the width for the ribbons), dimensionality typically dictates wide equilibrium distributions. These distributions are due to the necessary competition between the free energy gains in elongation versus the entropic gains associated with forming many species in solution. A well-known example is the wide distributions of effectively 1D rodlike micelles around some typical length [20]. A smaller yet still substantial spread is also displayed in the distribution of diameters of the final complexes, the closed nanotubes, which ranges between 70 and 100 nm [19].

Interestingly, at those regions where twisted ribbons transition into helical, most structures appear highly bent, suggesting that they are also considerably more flexible. This observation contrasts with nearly all twisted or helical ribbons, which are noticeably straight (compare, for example, Figs. 2 and 4). This feature may be interpreted as a reduction of the persistence length at the points of transition from one form to another and, hence, indicative of a lowering of the bending energies at that point. Indeed, Ghafouri and Bruinsma have suggested that near this critical point the ribbon should be highly flexible and show large orientational fluctuations [13]. This small persistence length and strong thermal orientational fluctuations were predicted to coincide with the second-order transition between forms.

In addition to class I complexes, images reveal a second class of ribbons (class II, orange symbols in Fig. 3), also exhibiting a steady, linear correlation of ribbon pitch (p) with ribbon width (w). About 8% of all structures belong to class II, and these display two distinctive characteristics. First, for a given ribbon width, the w/p ratio is much smaller than the values characteristics to class I structures ($0.039 < w/p < 0.075$ versus $0.08 < w/p < 0.23$). Second, with no exception, ribbons in class II do not undergo the structural transition and remain twisted even at widths larger than 40 nm (where class I exclusively forms helical ribbons). It thus appears that for each w/p ratio there will be a different characteristic ribbon width at

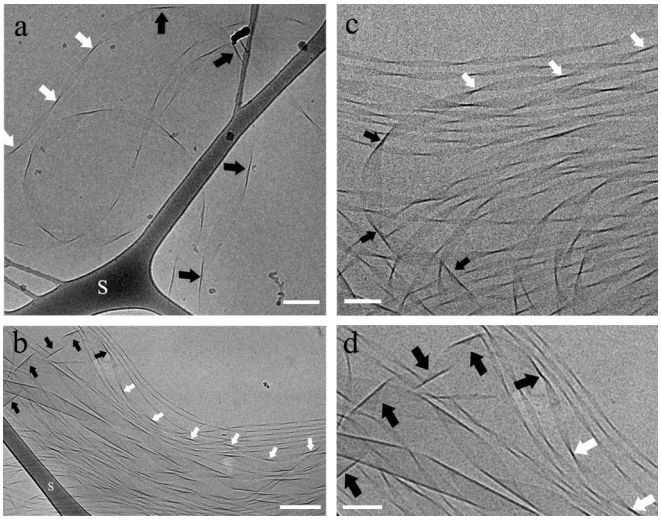

FIG. 4. Cryo-TEM images showing ribbons undergoing strong orientational fluctuations at regions where curvature changes from twisted (white arrows) to helical (black arrows) ribbons. Bar = 100 (a),(b) and 50 nm (c),(d). S in (a) and (b) marks the support film. (d) is a section of (c), shown at twice the magnification.

which the curvature type will vary. We suggest that class II structures, characterized by a much smaller w/p ratio (longer pitch for any given width, perhaps due to differences in molecular packaging), have not yet reached the critical width where a transition occurs. This finding may clarify the conundrum reported in previous investigations, whereby some systems seem locked in the twisted curvature state [10].

Slow kinetics of aggregation and the formation of metastable states on the way to full equilibrium at long times have been documented in other self-assembling chiral systems, for example, in self-assembling mixtures, for which the mechanism of chiral segregation has been proposed [21]. However, chiral segregation is not applicable to the case of a pure chiral material, as discussed here. Instead, we show that the kinetics is dominated by widening of the ribbons.

In conclusion, we have used cryo-TEM [22,23] to show unequivocal evidence for the link between ribbon width and its shape and morphology. We confirm the expectation from theory and simulations that ribbon shape is controlled by its width: Narrow chiral ribbons favor Gaussian saddle-like twisted curvature, while for wider ribbons (in our case, for class I $w > 35$ nm) the cylindrical curvature becomes favorable. This insight into twisted-to-cylindrical ribbon transition was possible due to the slow kinetics of the continuous widening process, which reaches the steady state only after several months, when the helically coiled ribbons close upon themselves into complete nanotubes.

D. D. thanks the Israel Science Foundation, The Russell Berrie Nanotechnology Institute (RBNI), and the Jewish Communities of Germany Research Fund for their generous support of the study. D. D and D. H. acknowledge the support of COST Action D43. The research was partly supported by the Israel Science Foundation (Grant No. 283/08 to A. M.).

*daniel@fh.huji.ac.il
†dganitd@tx.technion.ac.il

[1] I. Wickelgren, Science **280**, 517 (1998).
[2] J. H. Fuhrhop and W. Helfrich, Chem. Rev. **93**, 1565 (1993).
[3] T. Shimizu, M. Masuda, and H. Minamikawa, Chem. Rev. **105**, 1401 (2005).
[4] S. J. Hanley, J. F. Revol, L. Godbout, and D. G. Gray, Cellulose **4**, 209 (1997).
[5] D. S. Chung, G. B. Benedek, F. M. Konikoff, and J. M. Donovan, Proc. Natl. Acad. Sci. U.S.A. **90**, 11 341 (1993).
[6] F. M. Konikoff, D. S. Chung, J. M. Donovan, D. M. Small, and M. C. Carey, J. Clin. Invest. **90**, 1155 (1992).
[7] F. M. Konikoff, D. Danino, D. Weihs, M. Rubin, and Y. Talmon, Hepatology **31**, 261 (2000).
[8] J. V. Selinger and J. M. Schnur, Phys. Rev. Lett. **71**, 4091 (1993).
[9] M. Reches and E. Gazit, Science **300**, 625 (2003).
[10] R. Oda, I. Huc, M. Schmutz, S. J. Candau, and F. C. MacKintosh, Nature (London) **399**, 566 (1999).
[11] R. L. B. Selinger, J. V. Selinger, A. P. Malanoski, and J. M. Schnur, Phys. Rev. Lett. **93**, 158103 (2004).
[12] R. L. B. Selinger, J. V. Selinger, A. P. Malanoski, and J. M. Schnur, Chaos **14**, S3 (2004).
[13] R. Ghafouri and R. Bruinsma, Phys. Rev. Lett. **94**, 138101 (2005).
[14] S. Rotem and A. Mor, Biochim. Biophys. Acta **1788**, 1582 (2009).
[15] D. Danino, Y. Talmon, H. Levy, G. Beinert, and R. Zana, Science **269**, 1420 (1995).
[16] R. Zana (private communication).
[17] I. Radzishevsky, M. Krugliak, H. Ginsburg, and A. Mor, Antimicrob. Agents Chemother. **51**, 1753 (2007).
[18] I. S. Radzishevsky, T. Kovachi, Y. Porat, L. Ziserman, F. Zaknoon, D. Danino, and A. Mor, Chem. Biol. **15**, 354 (2008).
[19] L. Ziserman, H. Y. Lee, S. R. Raghavan, A. Mor, and D. Danino, J. Am. Chem. Soc. **133**, 2511 (2011).
[20] J. N. Israelachvili, D. J. Mitchell, and B. W. Ninham, J. Chem. Soc., Faraday Trans. 2 **72**, 1525 (1976).
[21] C. H. Chen and E. M. Terentjev, Langmuir **25**, 6717 (2009).
[22] D. Danino, A. Bernheim-Groswasser, and Y. Talmon, Colloids Surf. A **183**, 113 (2001).
[23] H. Cui, T. K. Hodgdon, E. W. Kaler, L. Abezgauz, D. Danino, M. Lubovsky, Y. Talmon, and D. J. Pochan, Soft Matter **3**, 945 (2007).